Developmental Cell
Matters Arising

The Adaptor Protein-1 μ1B Subunit Expands the Repertoire of Basolateral Sorting Signal Recognition in Epithelial Cells

Xiaoli Guo,[1] Rafael Mattera,[1] Xuefeng Ren,[1] Yu Chen,[1] Claudio Retamal,[2] Alfonso González,[2] and Juan S. Bonifacino[1,*]
[1]Cell Biology and Metabolism Program, *Eunice Kennedy Shriver* National Institute of Child Health and Human Development, National Institutes of Health, Bethesda, MD 20892, USA
[2]Departamento de Inmunología Clínica y Reumatología, Facultad de Medicina, Centro de Envejecimiento y Regeneración, Facultad de Ciencias Biológicas, Pontificia Universidad Católica de Chile, 6510260 Santiago, Chile
*Correspondence: bonifacinoj@helix.nih.gov
http://dx.doi.org/10.1016/j.devcel.2013.10.006

SUMMARY

An outstanding question in protein sorting is why polarized epithelial cells express two isoforms of the μ1 subunit of the AP-1 clathrin adaptor complex: the ubiquitous μ1A and the epithelial-specific μ1B. Previous studies led to the notion that μ1A and μ1B mediate basolateral sorting predominantly from the *trans*-Golgi network (TGN) and recycling endosomes, respectively. Using improved analytical tools, however, we find that μ1A and μ1B largely colocalize with each other. They also colocalize to similar extents with TGN and recycling endosome markers, as well as with basolateral cargoes transiting biosynthetic and endocytic-recycling routes. Instead, the two isoforms differ in their signal-recognition specificity. In particular, μ1B preferentially binds a subset of signals from cargoes that are sorted basolaterally in a μ1B-dependent manner. We conclude that expression of distinct μ1 isoforms in epithelial cells expands the repertoire of signals recognized by AP-1 for sorting of a broader range of cargoes to the basolateral surface.

INTRODUCTION

Epithelial cells are polarized into an apical domain that faces the exterior or lumen of body structures and a basolateral domain that contacts neighboring cells and the underlying basement membrane. The plasma membranes of the apical and basolateral domains have distinct protein compositions that endow them with specialized functions (Gonzalez and Rodriguez-Boulan, 2009; Cao et al., 2012). Protein sorting to the basolateral plasma membrane is mediated by signals in their cytosolic tails. Some basolateral signals fit canonical motifs similar to those of endocytic or lysosomal-targeting signals, including tyrosine-based (YXXØ or NPXY) (X is any amino acid, and Ø is a bulky hydrophobic amino acid) and dileucine-based ([DE]XXXL[LI]) signals (Bonifacino and Traub, 2003; Gonzalez and Rodriguez-Boulan, 2009). Others are unique sets of amino acids that do not conform to known canonical motifs (Gonzalez and Rodriguez-Boulan, 2009). In general, tyrosine- and dileucine-based signals bind to adaptor proteins (AP), including the heterotetrameric, clathrin-associated AP-1, AP-2, and AP-3 complexes and the non-clathrin-associated AP-4 complex (Bonifacino and Traub, 2003; Robinson, 2004). It was then natural to expect that basolateral sorting would involve recognition of a sorting signal by an AP complex, but the exact identity of this complex was initially unknown.

A key development in the search for a basolateral sorting adaptor was the discovery of μ1B, an isoform of the μ1 subunit of AP-1 that is specifically expressed in most, although not all, polarized epithelial cells in vertebrates (Ohno et al., 1999). AP-1 comprises four subunits named γ, β1, μ1, and σ1 (Figure 1A) (Robinson, 2004). Three of these subunits occur as multiple isoforms encoded by different genes, namely, γ1 and γ2, μ1A and μ1B, and σ1A, σ1B, and σ1C (Boehm and Bonifacino, 2001). With the exception of the epithelial-specific μ1B, all AP-1 subunit isoforms are widely expressed in different cell types. Combinatorial assembly of these subunits can give rise to at least 10 different AP-1 complexes (Mattera et al., 2011). Complexes containing either μ1A or μ1B are commonly referred to as AP-1A and AP-1B, respectively, notwithstanding that each of these designations encompasses several complexes that differ in their γ or σ1 isoforms. Functional analyses showed that μ1B is indeed required for basolateral sorting of various transmembrane proteins (Diaz et al., 2009; Fölsch et al., 1999; Gan et al., 2002; Sugimoto et al., 2002; Hase et al., 2013). Recent studies revealed that the ubiquitously expressed μ1A also contributes to basolateral sorting of some proteins, playing a complementary role to μ1B (Almomani et al., 2012; Carvajal-Gonzalez et al., 2012; Gravotta et al., 2012). These findings thus established AP-1, in both its AP-1A and AP-1B forms, as a critical regulator of basolateral sorting in polarized epithelial cells.

Despite progress in the elucidation of the mechanisms of basolateral sorting, an outstanding question remains: why did most epithelial cells evolve to express a specific AP-1 subunit isoform, μ1B, for the purpose of basolateral sorting? Over the past decade, several studies presented evidence that μ1A and μ1B have different intracellular localizations. Because μ1A and μ1B are highly homologous (~80% overall amino acid sequence identity in mammals) (Ohno et al., 1999), it was not possible to localize simultaneously both endogenous proteins

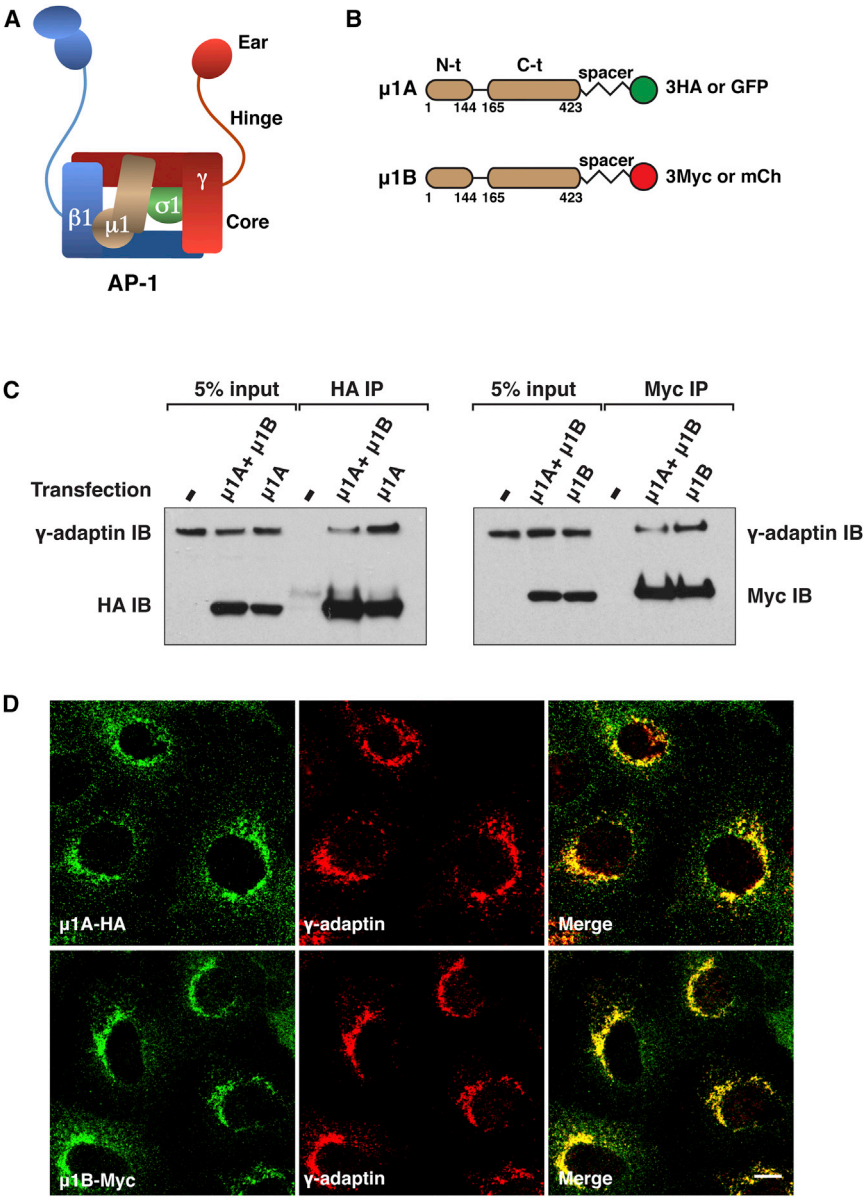

Figure 1. Expression of C-Terminally Tagged μ1A and μ1B in MDCK Cells

(A) Schematic representation of the AP-1 complex showing the γ, β1, μ1, and σ1 "adaptin" subunits and the core, hinge, and ear domains.

(B) Depiction of C-terminally tagged μ1A and μ1B constructs indicating the N-terminal (N-t) and C-terminal (C-t) domains, 10-amino-acid spacer (GSGSGGSGSG), three copies of the HA or Myc epitopes, or one copy of GFP or mCherry (mCh).

(C) MDCK cells stably expressing μ1A-HA, μ1B-Myc, or both isoforms were analyzed by immunoprecipitation (IP) with antibodies to the HA or Myc epitopes followed by SDS-PAGE and immunoblotting (IB) with antibodies to endogenous γ-adaptin and to the HA or Myc epitopes.

(D) MDCK cells stably expressing μ1A-HA or μ1B-Myc were double-immunostained for the HA or Myc epitopes and endogenous γ-adaptin. Scale bar, 10 μm. Quantification of colocalization is shown in Table 1.

by immunofluorescence and/or immunoelectron microscopy. Instead, their localization was inferred largely from expression of epitope-tagged proteins. Such studies concluded that μ1A and μ1B predominantly localize to the *trans*-Golgi network (TGN) and recycling endosomes (REs), respectively (Fölsch et al., 2001, 2003; Gan et al., 2002; Gravotta et al., 2012). Accordingly, μ1B must have evolved to enable basolateral sorting to take place from REs in most epithelial cells.

In the present study, we reassess the current understanding of the role of μ1B. Using a different tagging approach in conjunction with more advanced microscopy techniques, including superresolution and live-cell imaging, we find that μ1A and μ1B largely colocalize with each other as well as with the γ-adaptin subunit of AP-1. Their localization partially overlaps with that of TGN and RE markers and lies in the path of cargoes transiting to the cell surface in both biosynthetic and endocytic recycling routes. In contrast, μ1A and μ1B display distinct, albeit partially overlapping, cargo-recognition preferences. In particular, we demonstrate that noncanonical basolateral sorting signals from the μ1B-dependent cargo LDL receptor (LDLR) are preferentially recognized by μ1B. We conclude that expression of μ1B allows AP-1 to recognize a subset of cargo proteins that is not efficiently recognized by μ1A, thus expanding the range of proteins that are sorted to the basolateral plasma membrane.

RESULTS

C-Terminally Tagged μ1A and μ1B Colocalize with Each Other and with γ-Adaptin in Madin-Darby Canine Kidney Cells

To detect μ1A and μ1B, the mouse proteins were appended at their C termini with a 10-amino-acid spacer (GSGSGGSGSG, as per Argos, 1990) followed by three copies of the hemagglutinin (HA) or Myc epitopes, respectively (Figure 1B). Expression of the epitope-tagged proteins by transient transfection into nonpolarized Madin-Darby canine kidney (MDCK) epithelial cells showed localization of both proteins to a juxtanuclear structure characteristic of the TGN/REs in 39%–48% of the transfected cells, as analyzed by immunostaining and confocal fluorescence microscopy (Figures S1A and S1B available online). The rest of the transfected cells exhibited diffuse cytosolic staining or aggregates. Mouse μ1A and human μ1B constructs having an HA epitope inserted at an internal loop in their C-terminal domains displayed typical TGN/RE localization in 3%–17% of the transfected cells when analyzed under the same conditions (X.G. and J.S.B., unpublished data). Transient expression of C-terminally tagged μ1A and μ1B in MDCK cells

Table 1. Quantification of Colocalization

Proteins	Pearson's Coefficient	Manders' Coefficient (Threshold) tM1	tM2
μ1A-HA and γ-adaptin	0.79 ± 0.04	0.75 ± 0.06	0.74 ± 0.09
μ1B-Myc and γ-adaptin	0.81 ± 0.02	0.83 ± 0.06	0.76 ± 0.05
μ1A-HA and μ1B-Myc	0.80 ± 0.04	0.73 ± 0.07	0.75 ± 0.07
μ1A-HA and μ1B-Myc + Noco	0.74 ± 0.05	0.68 ± 0.05	0.64 ± 0.06
μ1B-Myc and Furin	0.68 ± 0.07	0.64 ± 0.05	0.65 ± 0.08
μ1B-Myc and Furin + Noco	0.43 ± 0.08	0.34 ± 0.05	0.42 ± 0.08
μ1B-Myc and TfR	0.62 ± 0.07[a]	0.66 ± 0.09	0.48 ± 0.09[b]
μ1B-Myc and TfR + Noco	0.38 ± 0.04	0.52 ± 0.14	0.28 ± 0.09
μ1B-Myc and SNX2	0.62 ± 0.04	0.65 ± 0.05	0.50 ± 0.08[b]
μ1B-Myc and EEA1	0.27 ± 0.05[c]	0.14 ± 0.04[c]	0.32 ± 0.08[c]

Quantification was performed with ImageJ and the JACoP plugin (Bolte and Cordelières, 2006) to determine the Pearson's coefficient and the Manders' coefficients tM1 (the fraction of colocalized intensity in channel 1 relative to total intensity in channel 1) and tM2 (the fraction of colocalized intensity in channel 2 relative to total intensity in channel 2). Scores are calculated for pixels above an automatically determined threshold for both channels, according to the algorithm of Costes et al. (2004). Values are the mean ± SD of 10–16 samples from three experiments. Statistical significance of differences was calculated by ANOVA followed by two-tailed Dunnett's test.

[a] $p < 0.05$ when compared to μ1B-Myc and Furin.

[b] $p < 0.01$ when compared to μ1B-Myc and Furin.

[c] $p < 0.01$ when compared to either μ1B-Myc and Furin, μ1B-Myc and TfR, or μ1B-Myc and SNX2.

resulted in their incorporation into the AP-1 complex, as assessed by coprecipitation with endogenous γ-adaptin; in contrast, μ1A and μ1B constructs with tags appended at their N termini did not assemble into AP-1 (Figure S1C). The better behavior of the C-terminally tagged constructs prompted us to use these in all subsequent experiments. Stable expression of μ1B-Myc in μ1B-deficient LLC-PK1 cells redirected the LDLR to the basolateral surface (Figure S1D) (Fölsch et al., 1999), indicating that this C-terminally tagged construct was functional.

We next developed stably transfected MDCK clones expressing C-terminally tagged μ1A-HA or μ1B-Myc, or both constructs together. Under these conditions, μ1A-HA and μ1B-Myc also coprecipitated with γ-adaptin, indicating that they were incorporated into the endogenous AP-1 complex (Figure 1C). Confocal fluorescence microscopy of stably transfected, nonpolarized cells expressing μ1A-HA and μ1B-Myc showed that both proteins extensively colocalized with endogenous γ-adaptin (Figure 1D) (Pearson's correlation coefficient [PCC], 0.79 for μ1A and 0.81 for μ1B; Table 1). μ1A-HA and μ1B-Myc also extensively colocalized with each other under normal culture conditions (Figure 2A) (PCC, 0.80; Table 1), as well as on dispersal of the TGN/REs by treatment with the microtubule-depolymerizing agent nocodazole (Figure 2B). This degree of colocalization approaches the maximum achievable for perfectly colocalized proteins, which in practice is less than 1 due to differences in fluorescent intensity and background staining in each channel (Bolte and Cordelières, 2006).

Because resolution in conventional fluorescence microscopy is limited by diffraction to ~200 nm (Betzig et al., 2006), we used superresolution structured illumination microscopy (SR-SIM), which has a resolution limit of ~100 nm. This technique was initially applied to nonpolarized, stably transfected MDCK clones expressing μ1A and μ1B that were C-terminally tagged with the same spacer (GSGSGGSGSG) and either green fluorescent protein (GFP) or mCherry, respectively (Figure 1B). At the higher resolution afforded by this technique, we also observed extensive colocalization of both proteins to juxtanuclear as well as peripheral structures (Figure 2C). Particularly in the cell periphery, it was easy to appreciate that μ1A and μ1B decorated the same constellations of particles (Figure 2C, lower panels).

MDCK cells can be grown as polarized monolayers on Transwell filters. Confocal fluorescence microscopy of such polarized cells showed localization of endogenous γ-adaptin to a subapical compartment characteristic of the TGN and REs (Figure 3A) (Apodaca et al., 1994; Barroso and Sztul, 1994; Brown et al., 2000; Ducharme et al., 2011). Analysis of polarized MDCK clones stably expressing μ1A-GFP and μ1B-mCherry showed that both proteins colocalized to the same subapical compartment in X-Y optical sections as well as X-Z and Y-Z projections (Figures 3B and 3C). Similar observations were made with SR-SIM of polarized cells (Figure 3D). These results indicated that tagged μ1A and μ1B colocalize regardless of the polarization state of the cells.

We also performed live-cell total internal reflection fluorescence (TIRF) microscopy to visualize the dynamics of structures containing μ1A-GFP and μ1B-mCherry located intracellularly up to 200 nm from the surface of nonpolarized MDCK cells (Figure 4; Movie S1). We observed that both proteins localized to the same structures (Figure 4A) and remained together as these structures moved throughout the evanescent field (Figures 4B and 4C; Movie S1) with velocities of ~1.5 μm/s (Figure 4D).

Finally, we examined the distribution of μ1A-HA and μ1B-Myc by subcellular fractionation of nonpolarized MDCK stable transfectants. Both proteins cosedimented on 40%–60% sucrose gradients in association with clathrin-coated vesicles (CCVs) containing clathrin and γ-adaptin (Figure S2A). The sedimentation behavior of these CCVs differed slightly from that of CCVs containing AP-2 α-adaptin and non-CCVs containing AP-4 ε-adaptin (Figure S2A). Immunoisolation of CCVs with anti-Myc followed by immunoblotting with anti-HA demonstrated association of both isoforms with the same CCVs (Figure S2B). Furthermore, μ1A-HA- and μ1B-Myc-containing membranes cosedimented with clathrin and γ-adaptin on 2%–18% iodixanol gradients (Figure S2C).

Taken together, these experiments indicated that the intracellular localizations of tagged μ1A and μ1B in MDCK cells are largely coincident under a variety of conditions, even when examined by methodologies that afford high spatial and temporal resolution. Both isoforms also colocalize with endogenous γ-adaptin to similar extents, consistent with uniform distribution of μ1 subunit isoforms among AP-1 complexes associated with cellular compartments.

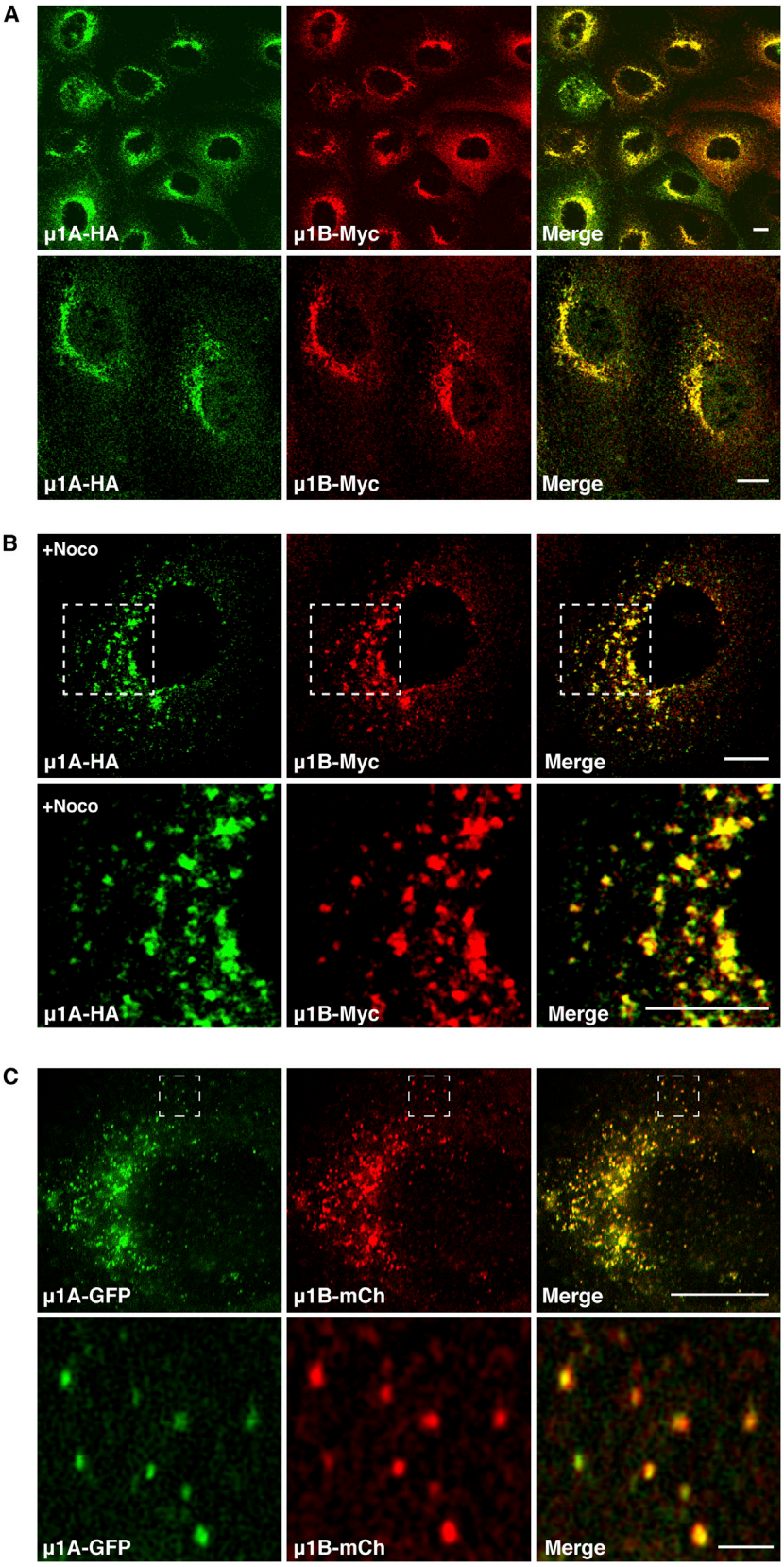

Figure 2. μ1A and μ1B Colocalize to the Same Juxtanuclear Compartment in Nonpolarized MDCK Cells

(A and B) MDCK cells stably coexpressing μ1A-HA and μ1B-Myc were left untreated (A) or treated with 4 μg/ml nocodazole (+Noco) (B) before immunostaining for the HA and Myc epitopes. In (A), cells are viewed at low (upper panels) or high magnification (lower panels). In (B), magnifications of the boxed regions are shown in the lower panels. Quantification of colocalization is shown in Table 1. Scale bars, 10 μm.

(C) MDCK cells stably coexpressing μ1A-GFP and μ1B-mCherry (mCh) were fixed with methanol at −20°C and viewed by SR-SIM. Magnifications of the boxed regions are shown in the lower panels. Scale bars, 10 μm in the upper panel and 2 μm in the lower panel.

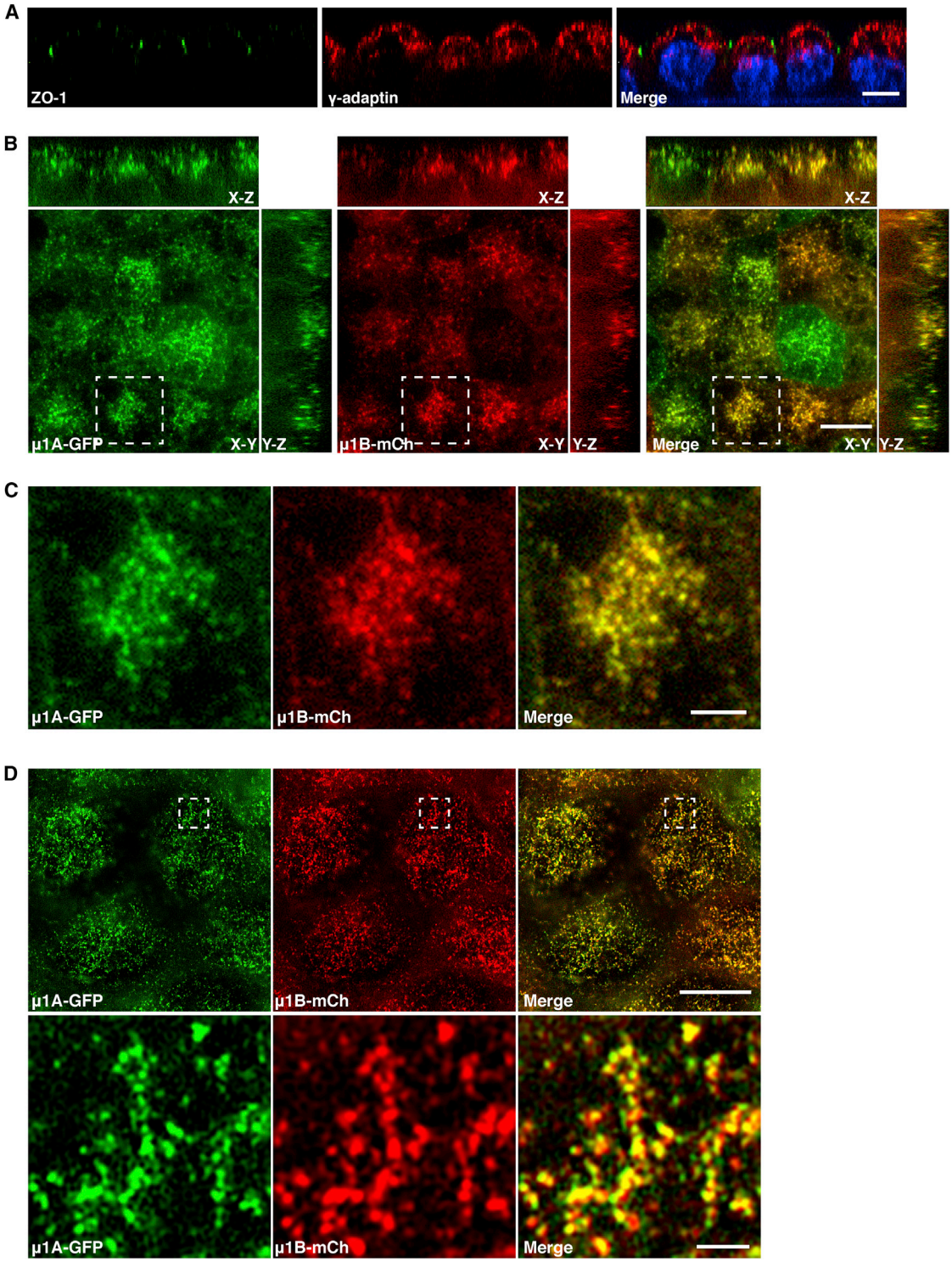

Figure 3. μ1A and μ1B Colocalize to a Subapical Compartment in Polarized MDCK Cells

(A) Polarized MDCK cells were fixed with 4% paraformaldehyde and double-immunostained for the tight junction marker ZO-1 and endogenous γ-adaptin. Nuclei were stained with DAPI. Scale bar, 10 μm.

(B and C) Polarized MDCK cells stably coexpressing μ1A-GFP and μ1B-mCherry (mCh) were fixed with methanol at −20°C and viewed with a spinning disk confocal microscope. Representative confocal images of the subapical region in X-Y sections are shown together with X-Z and Y-Z projections in (B). Magnifications of the boxed regions in (B) are shown in (C). Scale bars, 10 μm (B) and 3 μm (C).

(D) Polarized MDCK cells stably coexpressing μ1A-GFP and μ1B-mCherry were fixed with methanol at −20°C and viewed by SR-SIM. Magnifications of the boxed regions are shown in the lower panels. Scale bars, 10 μm in the upper panel and 1 μm in the lower panel.

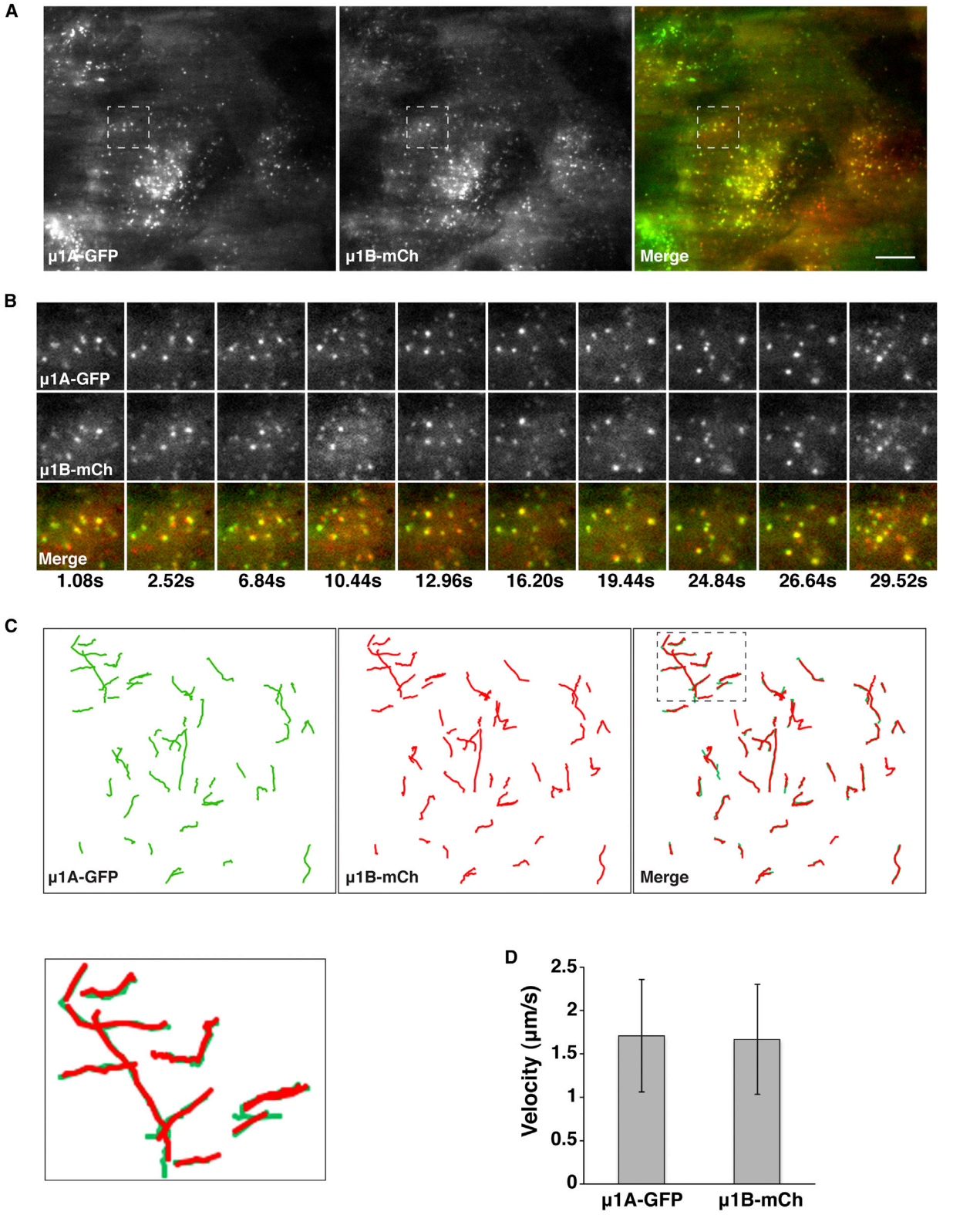

Figure 4. Colocalization of μ1A and μ1B in Live MDCK Cells

(A) TIRF microscopy of μ1A-GFP and μ1B-mCherry (mCh) stably coexpressed in live nonpolarized MDCK cells. Images of μ1A-GFP (150 ms exposure time) and μ1B-mCh (200 ms exposure time) were sequentially acquired within 200 nm of the plasma membrane. A single frame is shown.

(B) Magnifications of the boxed regions in (A) at different times.

(legend continued on next page)

Colocalization of μ1A and μ1B with TGN and RE Markers

To further characterize the structures with which tagged μ1A and μ1B are associated, we performed double-labeling for each isoform and endogenous organellar markers. Qualitative and quantitative analyses showed the same extent of colocalization of μ1A-HA and μ1B-Myc with various markers, in line with the colocalization of these isoforms with each other and with endogenous γ-adaptin (Table 1). Because of the similarity of the patterns, only the results for μ1B-Myc are shown (Figures 5A and 5B; Figure S3). The highest degree of colocalization was observed for μ1B-Myc with the TGN marker furin (Figure 5A) (PCC, 0.68; Table 1), although dispersal of the TGN with nocodazole revealed segregation of μ1B-Myc from furin within the same fragments (Figure 5A). There was a lower degree of colocalization with the early endosomal/RE marker TfR (Figure 5B) and the endosome-to-TGN recycling marker SNX2 (Figure S3) (PCC, 0.62 for both markers; Table 1) and no significant colocalization with the early endosomal marker, EEA1 (Figure S3) (PCC, 0.27; Table 1). From these experiments, we concluded that, at steady state, the localization of both tagged μ1A and μ1B partially overlaps with the TGN and REs but not significantly with early endosomes.

Transit of Biosynthetic and Endocytic Recycling Cargo through the AP-1 Compartment

We also examined the passage of the basolateral cargo protein LDLR through the AP-1 compartment in both biosynthetic and endocytic-recycling pathways in polarized MDCK cells. Because μ1A, μ1B and γ-adaptin largely colocalize with one another, only the results for μ1B are shown in Figures 5C and 5D. For analysis of biosynthetic transport, LDLR-GFP was expressed by nuclear microinjection of the corresponding plasmid (Cancino et al., 2007) into polarized MDCK cells stably expressing μ1B-mCherry. After microinjection, cells were incubated for 1 hr at 37°C to allow LDLR synthesis, followed by incubation for 2 hr at 20°C to arrest LDLR at the TGN (Cancino et al., 2007). Cells were then shifted to 37°C and imaged live at different times. We observed 34% colocalization of LDLR-GFP with μ1B-mCherry after the 20°C incubation (time 0 of chase) and 68% colocalization after 15 min of the shift to 37°C (Figure 5C). The degree of colocalization decreased to 15% after 50 min at 37°C, concomitant with appearance of LDLR-GFP at the plasma membrane (Figure 5C).

Analysis of endocytic recycling in polarized MDCK cells stably expressing μ1B-GFP was performed in cells transfected with an HA-LDLR plasmid (encoding the HA epitope in the extracellular domain). After internalization of an anti-HA antibody from the basolateral surface for 15 min at 37°C (time 0 of chase), cells were incubated for different times at 37°C to follow progression through REs. Cells were subsequently fixed and stained for the antibody to HA. We observed 31% colocalization of internalized HA-LDLR with μ1B-GFP at time 0, which increased to 51% at 15 min and decreased to 21% at 30 min of chase at 37°C (Figure 5D).

Taken together, these experiments indicated that AP-1 associates with compartments that intersect both biosynthetic and endocytic-recycling pathways, in agreement with the role of this complex in basolateral sorting in both routes (Cancino et al., 2007; Carvajal-Gonzalez et al., 2012; Fields et al., 2007; Fölsch et al., 1999; Gan et al., 2002; Gravotta et al., 2012).

Regulation of AP-1A and AP-1B Recruitment to Membranes by Arf Proteins

The association of AP-1 with TGN/RE membranes is regulated by members of the Arf family of GTPases (Stamnes and Rothman, 1993; Traub et al., 1993) and is sensitive to the Arf-GEF inhibitor brefeldin A (BFA) (Robinson and Kreis, 1992; Wong and Brodsky, 1992). Treatment with BFA caused dissociation of both AP-1A and AP-1B from the TGN/REs into the cytosol in stably transfected MDCK cells (Figure 6A), as previously shown for endogenous μ1B (Cancino et al., 2007). The Arf family is subdivided into classes I (Arf1, Arf3), II (Arf4, Arf5), and III (Arf6) (Donaldson and Jackson, 2011). The best characterized and most divergent members of this family are Arf1 and Arf6, which are regulated by BFA-sensitive and BFA-insensitive GEFs, respectively (Donaldson and Jackson, 2011). Consistent with the sensitivity of AP-1A and AP-1B to BFA, a dominant-negative Arf1 mutant (Arf1-T31N) displaced both complexes from TGN/REs to cytosol in MDCK cells, whereas an equivalent Arf6 mutant (Arf6-T27N) was less efficient (Figure 6B). We also used a glutathione S-transferase (GST) pull-down assay to compare the binding of recombinant AP-1A and AP-1B core complexes to different Arf family members in vitro. We found that both AP-1 variants bound to constitutively active forms of Arf1, Arf4, and Arf5 and, to a lesser extent, Arf6 (Figure 6C). Thus, AP-1A and AP-1B exhibit a similar pattern of regulation of membrane recruitment by Arf family members, preferring class I and II Arfs over Arf6.

Cargo Recognition Specificity of μ1B

If AP-1A and AP-1B have similar intracellular localizations and regulation by Arf family members, why then is μ1B required for sorting of a subset of cargoes to the basolateral plasma membrane? We hypothesized that μ1B might confer on AP-1 the ability to recognize cargoes that are not efficiently recognized by μ1A. To test this hypothesis, we screened the cytosolic tails of a large number of cargo proteins for interaction with μ1A and μ1B, using a yeast two-hybrid (Y2H) system (Ohno et al., 1995, 1996) with pGBKT7 as the bait vector. We found that most of the tails that tested positive in this assay interacted with both μ1A and μ1B (e.g., lysosomal-associated membrane protein 1 [LAMP1]) (Figure 7A). Some tails, however, interacted preferentially with either μ1A (e.g., the interleukin-6 receptor α chain [IL6R-α]) or μ1B (e.g., the interleukin-6 receptor β chain [IL6R-β] and the poliovirus receptor [PVR]) (Figure 7A). Notably, these preferential interactions correlated with the requirement of μ1B for basolateral sorting, since sorting of IL6R-α is μ1B independent (Takahashi et al., 2011), whereas sorting of IL6R-β (Takahashi et al., 2011) and PVR (Ohka et al., 2001) is μ1B dependent.

(C) A total of 50 trajectories for μ1A-GFP and 51 trajectories for μ1B-mCh were manually traced during 35.6 s of recording time. Magnification of the boxed region in the merged image is shown in the lower left panel.
(D) Quantification of the velocity of μ1A-GFP- and μ1B-mCh-labeled vesicles in the 35.6 s recording time. Values are the means ± SD calculated from the trajectories indicated in (C). Scale bar, 10 μm.

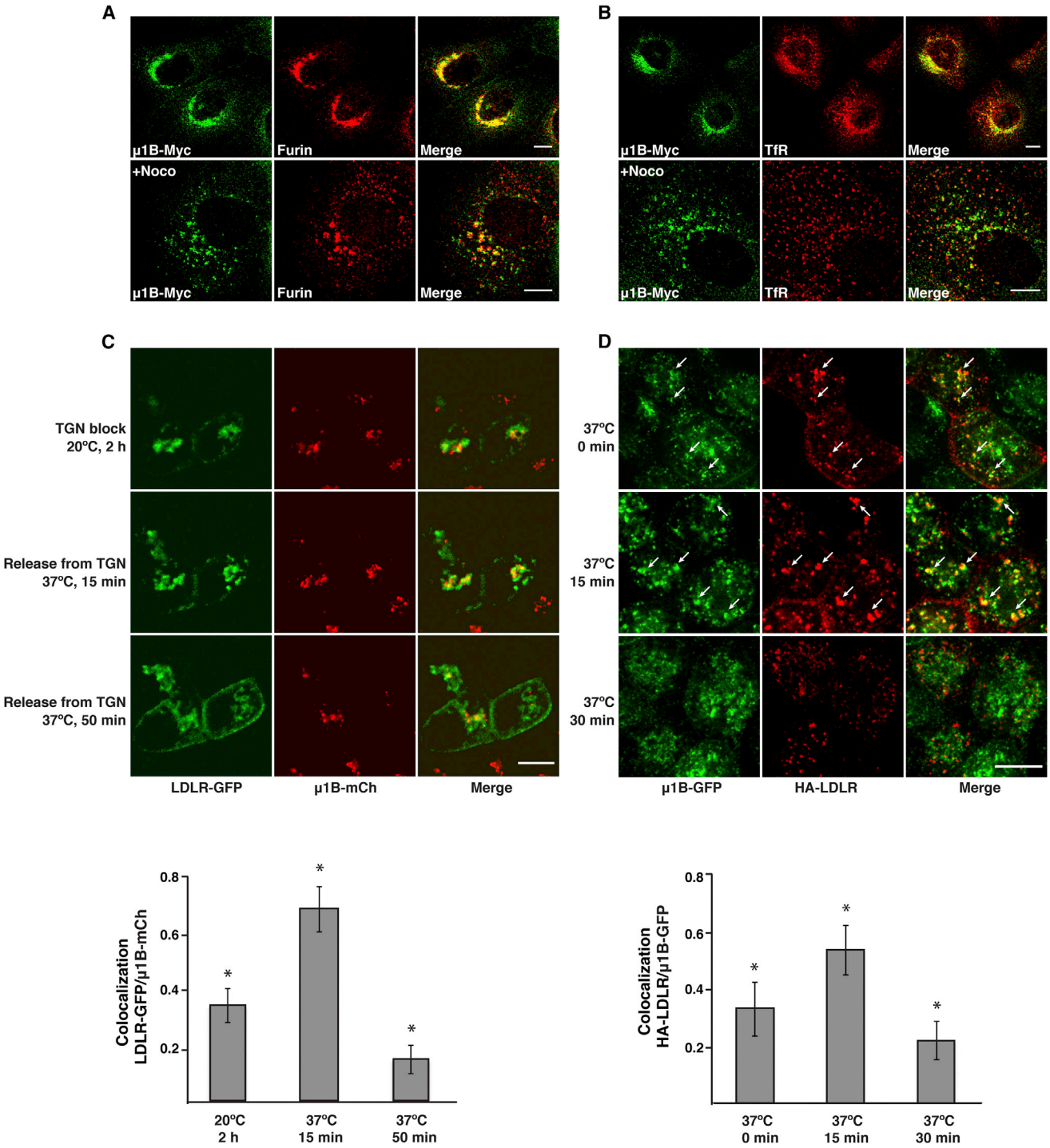

Figure 5. Colocalization of μ1B with Organellar Markers and Cargo Proteins

(A and B) Colocalization of μ1B with furin and TfR in nonpolarized MDCK cells. MDCK cells stably expressing μ1B-Myc were left untreated (upper panels) or treated with 4 μg/ml nocodazole (+Noco) for 80 min at 37°C (lower panels) before immunostaining for the Myc epitope and endogenous furin (A) or TfR (B). Scale bars, 10 μm. Quantification of colocalization is shown in Table 1.

(C and D) Colocalization of AP-1 with LDLR in biosynthetic and endocytic recycling routes in polarized MDCK cells. (C) Polarized MDCK cells stably expressing μ1B-mCherry (mCh) were microinjected with a plasmid encoding LDLR-GFP, incubated for 1 hr at 37°C, and then incubated for 2 hr at 20°C in the presence of cycloheximide (time 0) to arrest traffic at the TGN. Live cell imaging was started after release of the TGN block by shifting the temperature to 37°C. (D) Polarized MDCK cells stably expressing μ1B-GFP were transiently transfected with a plasmid encoding HA-LDLR. After 72 hr, cells were incubated with antibody to the HA epitope added to the basolateral medium for 15 min at 37°C, rinsed, and chased at 37°C for different times. Cells were then fixed with methanol at −20°C. Alexa

(legend continued on next page)

The cytosolic tail of a classical μ1B-dependent basolateral cargo, LDLR (Fölsch et al., 1999; Gravotta et al., 2012; Sugimoto et al., 2002), self-activated in this Y2H system. However, a fragment of this tail comprising residues 832–860 (Figure 7B) did not self-activate and showed preferential interaction with μ1B (Figures 7A and 7C). The LDLR tail contains two basolateral sorting signals: a proximal signal comprising a tyrosine residue (Y828) and an acidic patch (EDE 833-835), and a distal signal comprising two tyrosine residues (Y845 and Y847) and another acidic patch (EED 856-858) (Koivisto et al., 2001; Matter et al., 1992, 1993) (Figure 7B). The LDLR 832-860 fragment used in our Y2H assays comprised only the acidic cluster from the proximal signal and the complete distal signal (Figure 7B). Mutational analysis showed that all of these elements were required for interaction with μ1B (Figure 7D).

To confirm the LDLR tail interaction, we performed pull-down assays using the full-length LDLR tail fused to maltose-binding protein (MBP) and recombinant AP-1A and AP-1B core complexes tagged with GST. Assays were performed in the absence or presence of the constitutively active Arf1 Q71L mutant to test for interactions with the locked or open conformations of the AP-1 core, respectively (Ren et al., 2013). Pull-down with amylose beads followed by immunoblotting with antibody to GST showed that the LDLR tail bound AP-1B ~5-fold more avidly than AP-1A (Figures 7E and 7F). Binding to both complexes was activated by Arf1 Q71L and dependent on Y845 and Y847 in the LDLR tail (Figures 7E and 7F). These findings were consistent with those of the Y2H assays, with the added advantage that the higher sensitivity and lower background of the pull-down assay allowed detection of a weaker interaction of the LDLR tail with AP-1A.

Taken together, these analyses demonstrated a strong correlation between basolateral sorting and preferential interaction with μ1B for at least three cargo proteins (i.e., IL6R-β, PVR, and LDLR), indicating that μ1B exists to sort cargoes that are not efficiently recognized by μ1A.

DISCUSSION

Several subunits of the heterotetrameric AP-1, AP-2, and AP-3 complexes occur as multiple isoforms encoded by different genes. Although significant progress has been made in the elucidation of the specific functions of AP complex subunits, the purpose served by the existence of subunit isoforms remains obscure. In the case of AP-1, the μ1A and μ1B subunit isoforms were proposed to specify localization of the complex to different intracellular compartments. We reassessed this notion using improved analytical tools, including (1) a way to tag μ subunits by placement of a spacer and epitope tags or fluorescent proteins at the C terminus, (2) expression of the tagged proteins by stable cotransfection in nonpolarized and polarized MDCK cells, (3) microscopic techniques with high spatial (SR-SIM) and temporal (live-cell TIRF) resolution. In contrast to previous studies, we found that the intracellular localizations of μ1A and μ1B in MDCK cells are highly coincident under a variety of conditions. Thus, the presence of a specific μ1 subunit isoform does not appear to confer distinct localization on the AP-1 complex.

The μ1A and μ1B isoforms, as well as the γ subunit of AP-1, localize to a juxtanuclear compartment that partially overlaps with both the TGN and REs, as previously shown for the generic AP-1 complex (Delevoye et al., 2009; Eskelinen et al., 2002; Futter et al., 1998; Klumperman et al., 1993; Peden et al., 2004; Robinson, 1990). We could not determine the exact localization of μ1A and μ1B by immunoelectron microscopy because of the low density of labeling of both epitope-tagged isoforms (M. Jarnik and J.S.B., unpublished data). However, analysis of the biosynthetic transport of newly synthesized LDLR indicated that this compartment lies immediately distal to the TGN, as operationally defined by maximum colocalization of LDLR with AP-1 shortly after release from a 20°C block, and is accessible to endocytosed LDLR, as shown by a peak of colocalization at 15 min after internalization.

The colocalization of μ1A and μ1B is consistent with the fact that the main determinants of AP-1 localization to the TGN/REs reside within the γ and β1 subunits of the complex. These determinants include binding sites for Arf family GTPases on the γ and β1 subunits (Austin et al., 2002; Ren et al., 2013) and for phosphatidylinositol 4-phosphate on the γ subunit (Heldwein et al., 2004; Wang et al., 2003). Since μ1A and μ1B share the same γ and β1 subunits in the AP-1 complex, it is logical that they exhibit similar overall localizations within cells. Phosphatidylinositol 3,4,5-trisphosphate, a phosphoinositide that is enriched at the plasma membrane and REs, has been functionally implicated in μ1B-dependent sorting (Fields et al., 2010). It remains to be determined, however, if this phosphoinositide binds directly and preferentially to μ1B. The colocalization of AP-1A and AP-1B supports their previously reported functions at both the TGN and REs. Indeed, although AP-1A and AP-1B were shown to mediate sorting predominantly at the TGN and REs, respectively, AP-1A also participates in endosomal sorting events (Delevoye et al., 2009; Hirst et al., 2012) and AP-1B can promote export from the TGN under some conditions (Gravotta et al., 2012). Moreover, μ1B can substitute for μ1A in the sorting of mannose 6-phosphate receptors between endosomes and the TGN (Eskelinen et al., 2002). Our findings do not rule out that AP-1A and AP-1B could function preferentially in biosynthetic or recycling pathways depending on the cargo or other regulatory inputs. Since cargo binding promotes membrane recruitment of AP-1 through stabilization of the active conformation of the AP-1 core (Lee et al., 2008; Ren et al., 2013), the local availability of specific cargoes could determine the exact compartment where each AP-1 variant exerts its function.

The μ subunits of AP complexes mediate cargo recognition through interaction with specific sorting signals. The μ1A isoform, in particular, has long been known to bind YXXØ signals (Ohno et al., 1995, 1996). Several studies also showed interactions of μ1B with the cytosolic tails of PVR (Ohka et al., 2001),

555-conjugated goat anti-mouse secondary antibody was used to detect HA antibody, and μ1B-GFP fluorescence was used to visualize AP-1 complex. Arrows point to selected structures where internalized HA-LDLR colocalizes with μ1B-GFP. Bar graphs show the Manders' coefficients for colocalization of LDLR-GFP with μ1B-mCh (mean ± SD, n = 6–7) in (C) and of HA-LDLR with μ1B-GFP (mean ± SD, n = 13–15) in (D) at the different time points. *$p < 0.01$ for all comparisons in each graph (ANOVA followed by two-tailed Dunnett's test). Scale bars, 10 μm.

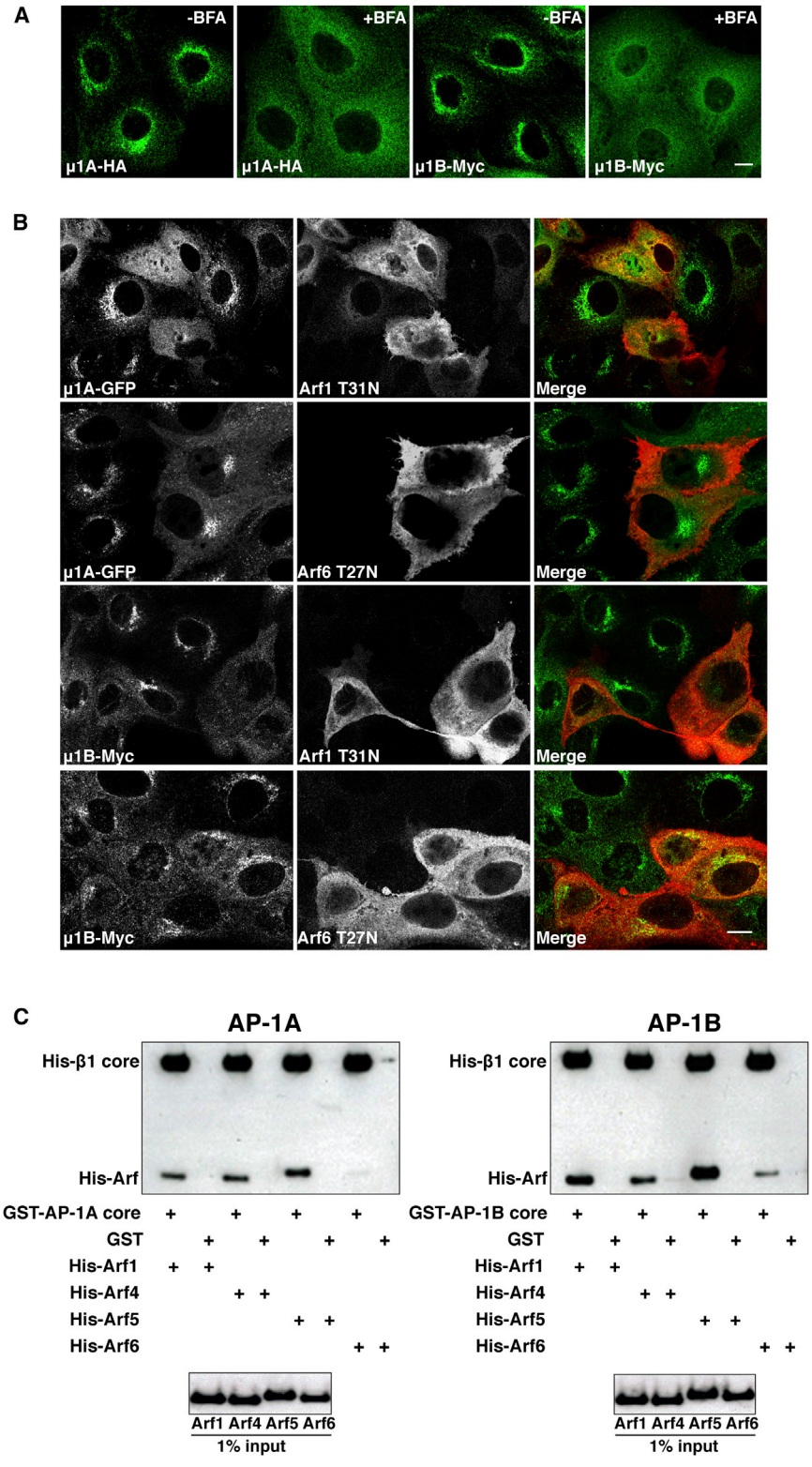

Figure 6. Similar Patterns of AP-1A and AP-1B Regulation by Arf Proteins

(A) MDCK cells stably expressing μ1A-HA or μ1B-Myc were left untreated or treated with 5 μg/ml BFA for 15 min at 37°C, before immunostaining with antibodies to the HA or Myc epitopes. Scale bar, 10 μm.

(B) MDCK cells stably expressing μ1A-GFP or μ1B-Myc were transfected with plasmids encoding dominant-negative HA-tagged Arf1 T31N or Arf6 T27N mutants. At 24 hr after transfection, μ1A-GFP was detected by GFP fluorescence, and μ1B-Myc or Arf-HA was detected by immunostaining with antibodies to the Myc and HA epitopes. Scale bar, 10 μm.

(C) Purified GST-His-tagged AP-1A or AP-1B core complex was incubated with His-tagged Arf1, Arf4, Arf5, or Arf6 constitutively active (QL) mutants. Bound proteins were isolated on glutathione-Sepharose beads and analyzed by SDS-PAGE and immunoblotting with antibodies to the His tag. GST was used as a negative control.

TGN38 (Fields et al., 2007), TfR (Fields et al., 2007; Gravotta et al., 2012) and CAR (Carvajal-Gonzalez et al., 2012), which are at least partly dependent on YXXØ signals. The analyses presented here reveal a strong correlation between preferential interactions with μ1B (Figure 7A) and basolateral sorting dependent on μ1B for at least three cargoes: IL6R-β, PVR, and LDLR (Doumanov et al., 2006; Fölsch et al., 1999; Gravotta et al., 2012; Martens et al., 2000; Ohka et al., 2001; Sugimoto et al., 2002; Takahashi et al., 2011). In further support of this correlation, a cargo that interacts specifically with μ1A, IL6R-α (Figure 7A), does not require μ1B for basolateral sorting (Takahashi et al., 2011). We also dissected the sequences in the LDLR tail that are required for interaction with μ1B and found that they correspond to the noncanonical tyrosine-based signals and clusters of acidic residues that were previously implicated in basolateral sorting (Koivisto et al., 2001; Matter et al., 1992, 1993). Together with the previous observation that interaction of the TfR tail with μ1B partly relies on a GDNS amino acid signal (Gravotta et al., 2012; Odorizzi and Trowbridge, 1997), our findings indicate that μ1B is capable of recognizing noncanonical signals in addition to YXXØ signals. From these observations, we conclude that direct and preferential recognition by μ1B underlies the requirement of this isoform for basolateral sorting of a subset of cargoes.

The aforementioned considerations lead us to propose that expression of μ1B in polarized epithelial cells expands the repertoire of cargoes that are recognized by AP-1. The ubiquitous μ1A isoform is capable of performing basolateral sorting, but μ1B makes this sorting more efficient for some cargoes (Gravotta et al.,

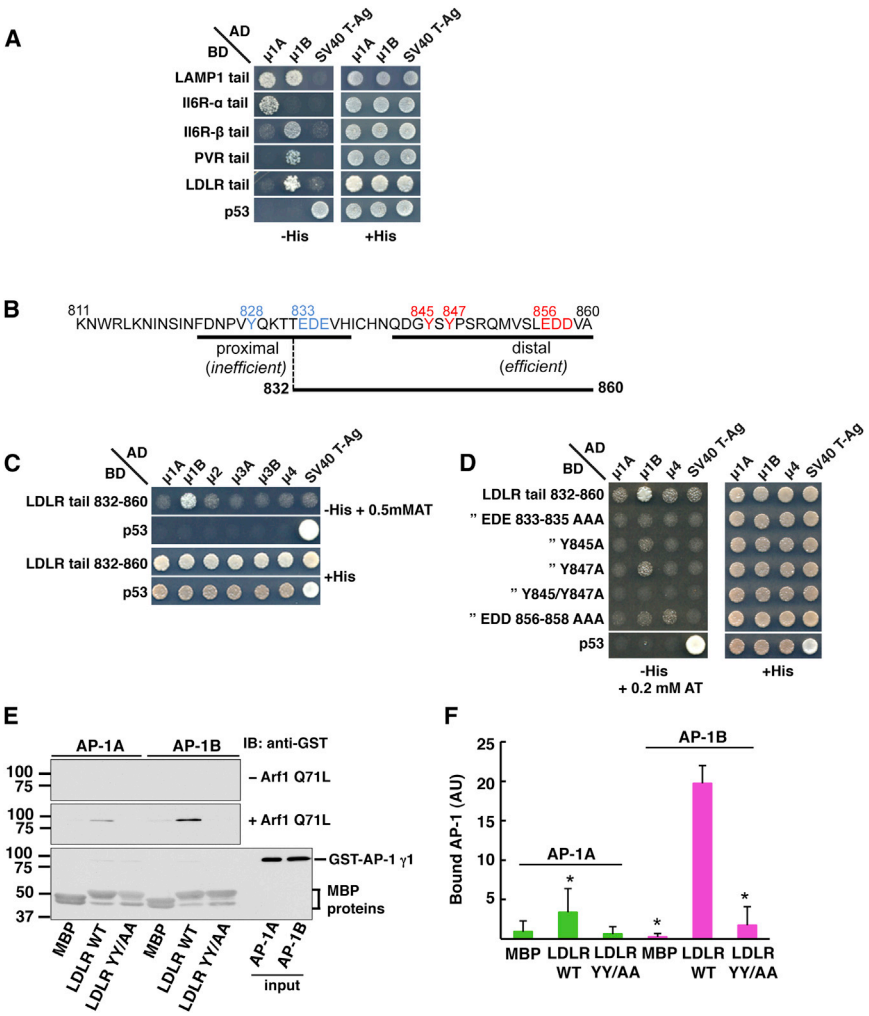

Figure 7. Differential Recognition of Basolateral Cargoes by AP-1 μ1A and μ1B

(A) Y2H analysis of the interaction of the LAMP1 tail (residues 406–417), IL6R-α (residues 387–468), IL6R-β tail (residues 642–918), PVR tail (residues 368–417), and LDLR tail (residues 832–860) with μ1A and μ1B. Growth on plates lacking histidine (-His) is indicative of interactions. Assays with Il6R-β and LDLR tails were performed on -His plates containing 3 mM or 0.5 mM 3-amino-1,2,4-triazole (AT) respectively, to minimize self-activation and nonspecific interactions.

(B) Amino acid sequence of the LDLR cytosolic tail showing proximal and distal basolateral signals. Tyrosine residues and acidic clusters important for the proximal and distal basolateral sorting determinants are highlighted in blue and red, respectively. The LDLR cytosolic tail construct 832-860 used in the Y2H analysis comprises the acidic cluster from the proximal determinant and the entire distal basolateral determinant.

(C) Y2H analysis of the interaction of LDLR 832-860 with μ subunits from AP-1, AP-2, AP-3, and AP-4.

(D) Y2H analysis of the interaction of LDLR tail mutants. Images shown here, as well as in (A) and (C), are composites of panels from the same experiments.

(E) Pull-down of GST-tagged-AP-1A and -AP-1B core complexes by MBP-LDLR tail wild-type (WT) or Y845A/Y847A (YY/AA) fusions immobilized on to amylose resin. Incubations were carried out in the absence or presence of Arf1 Q71L mutant (upper and middle panels, respectively). Bound proteins were eluted and analyzed by SDS-PAGE and immunoblotting with anti-GST. MBP was used as negative control. The lower panel shows the MBP proteins and the AP-1A/AP-1B input used in the assay.

(F) Densitometric analysis of immunoblots from three independent pull-downs of AP-1A/AP-1B by MBP-LDLR tail fusions. Results are the means ± SD of densitometric arbitrary units (AU). Statistical significance was analyzed by one-way ANOVA followed by two-tailed Dunnett's test. *$p < 0.01$, when compared to pull-down of AP-1B by MBP-LDLR tail WT.

2012; Carvajal-Gonzalez et al., 2012). In the absence of μ1B, some basolateral cargoes adopt a nonpolarized distribution between the basolateral and apical surfaces. Cells also lose some of their polarized features (Fölsch et al., 1999; Sugimoto et al., 2002). However, they do not become completely nonpolarized. Indeed, some epithelial cells such as renal proximal tubule cells do not express μ1B (Schreiner et al., 2010) but nonetheless exhibit differentiated basolateral and apical plasma membrane domains. Such cells may also sort specific cargoes to the basolateral surface in both biosynthetic and endocytic pathways. What renal proximal tubule cells do exhibit is apical expression of some cargoes such as the LDLR, in contrast to μ1B-expressing epithelial cells such as enterocytes where the LDLR is exclusively basolateral (Pathak et al., 1990; Hase et al., 2013). Thus, expression of μ1B acts as a cell-type-specific switch to exclude a subset of transmembrane proteins from the apical surface.

In sum, our results indicate that expression of distinct μ1 subunit isoforms in polarized epithelial cells diversifies the signal-recognition specificity of the AP-1 complex, allowing for efficient and regulated sorting of a broader set of cargoes to the basolateral surface.

EXPERIMENTAL PROCEDURES

μ1A and μ1B Constructs

cDNAs encoding mouse μ1A and μ1B appended at the N or C terminus with a 10-amino-acid spacer sequence (GSGSGGSGSG) and three copies of the HA (μ1A-HA) or Myc epitopes (μ1B-Myc) were cloned into pCI-neo (Promega) or pcDNA3.1/hygro(+) (Invitrogen/Life Technologies), respectively. cDNAs encoding mouse μ1A and μ1B with the 10-amino-acid spacer and GFP (μ1A-GFP and μ1B-GFP) or mCherry (μ1B-mCherry) were made by cloning into pEGFP-N1 or pmCherry-N1 (Clontech). The μ1A-GFP construct was also subcloned into pcDNA3.1/hygro(+).

Cell Culture, Polarization, and Transfection

MDCK (MDCK-II strain, Sigma-Aldrich) cells were cultured at 37°C in minimum essential medium (Cellgro) supplemented with 10% fetal bovine serum, 2 mM glutamine, 100 U/ml penicillin, and 100 μg/ml streptomycin. Cells were transfected using Lipofectamine 2000 (Invitrogen/Life Technologies). Stably transfected cell lines were selected with 800 μg/ml G418 (Cellgro) or 200 μg/ml hygromycin (Cellgro). For polarized culture, cells were plated on 0.4-μm

Transwell filters (Costar) by seeding 3 × 10^5 cells per 12-mm filter. After an initial attachment period of 6 hr, excess cells were removed and monolayers were fed daily with fresh medium.

Fluorescence Microscopy and Image Analysis

Fluorescence images of fixed nonpolarized MDCK cells expressing different constructs were obtained using a confocal microscope (SP5, Leica; or 710, Zeiss). Fixed polarized MDCK cells expressing different constructs were imaged using a Marianas spinning disc microscope (Intelligent Imaging Innovations). Digital images were acquired with an Evolve electron-multiplying charge-coupled device (EM-CCD) camera (Photometrics). TIRF microscopy images were acquired using a True MultiColor Laser TIRF microscope system (Leica) equipped with a high-speed EM-CCD camera (C9100-13; Hamamatsu Photonics, Hamamatsu, Japan), a HCX Plan-Apochromat 100× objective lens (NA 1.46; Leica), a C-mount 1.6× expansion lens, and Leica AF6000 software. During imaging, cells were kept in phenol-red-free Dulbecco's modified Eagle's medium (Invitrogen/Life Technologies) at 37°C. For SR-SIM, imaging was performed on a Zeiss Elyra system. Image analysis was performed with ImageJ (National Institutes of Health). Quantitative colocalization analysis was performed with the JACoP plugin (Bolte and Cordelières, 2006) and expressed as three parameters: the Pearson's correlation coefficient and the Manders' coefficients tM1 for channel 1 and tM2 for channel 2. For images with high background fluorescence, background was subtracted using a region of interest (ROI) outside cells and the "subtract background from ROI" routine in ImageJ. For each condition, more than 10 cells from three different cell cultures were analyzed. For μ1 vesicle tracking, the Manual Tracking plugin of ImageJ was used to maximize fidelity of tracking. To calculate the speed of μ1 vesicles, the dynamicity parameters were extracted using the same plugin.

Assays for Biosynthetic Transport and Internalization of the LDLR

For analysis of biosynthetic transport of the LDLR, polarized MDCK cells stably expressing μ1B-mCherry and grown on cover glasses were microinjected with pCB6-LDLR-GFP using back-loaded glass capillaries and an Eppendorf NI-2 micromanipulator coupled to an Eppendorf Femtojet microinjector. After 1 hr of protein synthesis at 37°C, cells were incubated for 2 hr at 20°C in the presence of cycloheximide to accumulate newly synthesized LDLR-GFP at the TGN. Cells were then shifted to 37°C using a perfusion-open-close thermal-controlled chamber (Leica) for time-lapse imaging in vivo, with an inverted microscope (Leica DMI6000b, AF7000, Leica Microsystems) and a HCX 63× glycerin immersion lens. XYZT series were taken using the LAS AF software and an iXon 887 EM-CCD camera (Andor). Images were processed and analyzed with Huygens Essential (ZVI) software. All images from a single experiment were acquired under identical settings (16 bits; 1,024 × 1,024 pixels, and the same exposure times, avoiding signal saturation) and analyzed after three-dimensional deconvolution.

For analysis of endocytic transport of the LDLR, polarized MDCK cells stably expressing μ1B-GFP and grown on Transwell filters to 100% confluence were transiently transfected with a plasmid encoding HA-LDLR. After 72 hr, mouse anti-HA (Covance) was added to the basolateral medium, and cells were incubated for 15 min at 37°C, washed with PBS, chased in complete medium at 37°C, and fixed with methanol at −20°C. Internalized antibody was detected by Alexa 555-conjugated goat anti-mouse secondary antibody. Fluorescence images were obtained with a Marianas spinning disc microscope, and digital images were acquired with an Evolve EM-CCD camera. Quantitative colocalization analysis was performed with ImageJ and the JACoP plugin.

Additional Methods

Additional information on DNA constructs, immunoprecipitation and immunofluorescence, subcellular fractionation, expression and purification of recombinant proteins, and pull-down and yeast two-hybrid assays is provided in the Supplemental Experimental Procedures.

SUPPLEMENTAL INFORMATION

Supplemental information includes Supplemental Experimental Procedures, three figures, and one movie and can be found with this article online at http://dx.doi.org/10.1016/j.devcel.2013.10.006.

ACKNOWLEDGMENTS

We thank X. Zhu and N. Tsai for technical assistance; M. Jarnik for electron microscopy analysis; and G. Bu, K. Matter, and J. Donaldson for gifts of reagents. This work was funded by the Intramural Program of the *Eunice Kennedy Shriver* National Institute of Child Health and Human Development and the Basal Financial Program, grant PFB12/2007, of CONICYT (C.R. and A.G.).

Received: December 26, 2012
Revised: July 15, 2013
Accepted: October 10, 2013
Published: November 11, 2013

REFERENCES

Almomani, E.Y., King, J.C., Netsawang, J., Yenchitsomanus, P.T., Malasit, P., Limjindaporn, T., Alexander, R.T., and Cordat, E. (2012). Adaptor protein 1 complexes regulate intracellular trafficking of the kidney anion exchanger 1 in epithelial cells. Am. J. Physiol. Cell Physiol. *303*, C554–C566.

Apodaca, G., Katz, L.A., and Mostov, K.E. (1994). Receptor-mediated transcytosis of IgA in MDCK cells is via apical recycling endosomes. J. Cell Biol. *125*, 67–86.

Argos, P. (1990). An investigation of oligopeptides linking domains in protein tertiary structures and possible candidates for general gene fusion. J. Mol. Biol. *211*, 943–958.

Austin, C., Boehm, M., and Tooze, S.A. (2002). Site-specific cross-linking reveals a differential direct interaction of class 1, 2, and 3 ADP-ribosylation factors with adaptor protein complexes 1 and 3. Biochemistry *41*, 4669–4677.

Barroso, M., and Sztul, E.S. (1994). Basolateral to apical transcytosis in polarized cells is indirect and involves BFA and trimeric G protein sensitive passage through the apical endosome. J. Cell Biol. *124*, 83–100.

Betzig, E., Patterson, G.H., Sougrat, R., Lindwasser, O.W., Olenych, S., Bonifacino, J.S., Davidson, M.W., Lippincott-Schwartz, J., and Hess, H.F. (2006). Imaging intracellular fluorescent proteins at nanometer resolution. Science *313*, 1642–1645.

Boehm, M., and Bonifacino, J.S. (2001). Adaptins: the final recount. Mol. Biol. Cell *12*, 2907–2920.

Bolte, S., and Cordelières, F.P. (2006). A guided tour into subcellular colocalization analysis in light microscopy. J. Microsc. *224*, 213–232.

Bonifacino, J.S., and Traub, L.M. (2003). Signals for sorting of transmembrane proteins to endosomes and lysosomes. Annu. Rev. Biochem. *72*, 395–447.

Brown, P.S., Wang, E., Aroeti, B., Chapin, S.J., Mostov, K.E., and Dunn, K.W. (2000). Definition of distinct compartments in polarized Madin-Darby canine kidney (MDCK) cells for membrane-volume sorting, polarized sorting and apical recycling. Traffic *1*, 124–140.

Cancino, J., Torrealba, C., Soza, A., Yuseff, M.I., Gravotta, D., Henklein, P., Rodriguez-Boulan, E., and González, A. (2007). Antibody to AP1B adaptor blocks biosynthetic and recycling routes of basolateral proteins at recycling endosomes. Mol. Biol. Cell *18*, 4872–4884.

Cao, X., Surma, M.A., and Simons, K. (2012). Polarized sorting and trafficking in epithelial cells. Cell Res. *22*, 793–805.

Carvajal-Gonzalez, J.M., Gravotta, D., Mattera, R., Diaz, F., Perez Bay, A., Roman, A.C., Schreiner, R.P., Thuenauer, R., Bonifacino, J.S., and Rodriguez-Boulan, E. (2012). Basolateral sorting of the coxsackie and adenovirus receptor through interaction of a canonical YXXPhi motif with the clathrin adaptors AP-1A and AP-1B. Proc. Natl. Acad. Sci. USA *109*, 3820–3825.

Costes, S.V., Daelemans, D., Cho, E.H., Dobbin, Z., Pavlakis, G., and Lockett, S. (2004). Automatic and quantitative measurement of protein-protein colocalization in live cells. Biophys. J. *86*, 3993–4003.

Delevoye, C., Hurbain, I., Tenza, D., Sibarita, J.B., Uzan-Gafsou, S., Ohno, H., Geerts, W.J., Verkleij, A.J., Salamero, J., Marks, M.S., and Raposo, G. (2009). AP-1 and KIF13A coordinate endosomal sorting and positioning during melanosome biogenesis. J. Cell Biol. *187*, 247–264.

Diaz, F., Gravotta, D., Deora, A., Schreiner, R., Schoggins, J., Falck-Pedersen, E., and Rodriguez-Boulan, E. (2009). Clathrin adaptor AP1B controls adenovirus infectivity of epithelial cells. Proc. Natl. Acad. Sci. USA *106*, 11143–11148.

Donaldson, J.G., and Jackson, C.L. (2011). ARF family G proteins and their regulators: roles in membrane transport, development and disease. Nat. Rev. Mol. Cell Biol. *12*, 362–375.

Doumanov, J.A., Daubrawa, M., Unden, H., and Graeve, L. (2006). Identification of a basolateral sorting signal within the cytoplasmic domain of the interleukin-6 signal transducer gp130. Cell. Signal. *18*, 1140–1146.

Ducharme, N.A., Ham, A.J., Lapierre, L.A., and Goldenring, J.R. (2011). Rab11-FIP2 influences multiple components of the endosomal system in polarized MDCK cells. Cell. Logist. *1*, 57–68.

Eskelinen, E.L., Meyer, C., Ohno, H., von Figura, K., and Schu, P. (2002). The polarized epithelia-specific mu 1B-adaptin complements mu 1A-deficiency in fibroblasts. EMBO Rep. *3*, 471–477.

Fields, I.C., King, S.M., Shteyn, E., Kang, R.S., and Fölsch, H. (2010). Phosphatidylinositol 3,4,5-trisphosphate localization in recycling endosomes is necessary for AP-1B-dependent sorting in polarized epithelial cells. Mol. Biol. Cell *21*, 95–105.

Fields, I.C., Shteyn, E., Pypaert, M., Proux-Gillardeaux, V., Kang, R.S., Galli, T., and Fölsch, H. (2007). v-SNARE cellubrevin is required for basolateral sorting of AP-1B-dependent cargo in polarized epithelial cells. J. Cell Biol. *177*, 477–488.

Fölsch, H., Ohno, H., Bonifacino, J.S., and Mellman, I. (1999). A novel clathrin adaptor complex mediates basolateral targeting in polarized epithelial cells. Cell *99*, 189–198.

Fölsch, H., Pypaert, M., Schu, P., and Mellman, I. (2001). Distribution and function of AP-1 clathrin adaptor complexes in polarized epithelial cells. J. Cell Biol. *152*, 595–606.

Fölsch, H., Pypaert, M., Maday, S., Pelletier, L., and Mellman, I. (2003). The AP-1A and AP-1B clathrin adaptor complexes define biochemically and functionally distinct membrane domains. J. Cell Biol. *163*, 351–362.

Futter, C.E., Gibson, A., Allchin, E.H., Maxwell, S., Ruddock, L.J., Odorizzi, G., Domingo, D., Trowbridge, I.S., and Hopkins, C.R. (1998). In polarized MDCK cells basolateral vesicles arise from clathrin-gamma-adaptin-coated domains on endosomal tubules. J. Cell Biol. *141*, 611–623.

Gan, Y., McGraw, T.E., and Rodriguez-Boulan, E. (2002). The epithelial-specific adaptor AP1B mediates post-endocytic recycling to the basolateral membrane. Nat. Cell Biol. *4*, 605–609.

Gonzalez, A., and Rodriguez-Boulan, E. (2009). Clathrin and AP1B: key roles in basolateral trafficking through trans-endosomal routes. FEBS Lett. *583*, 3784–3795.

Gravotta, D., Carvajal-Gonzalez, J.M., Mattera, R., Deborde, S., Banfelder, J.R., Bonifacino, J.S., and Rodriguez-Boulan, E. (2012). The clathrin adaptor AP-1A mediates basolateral polarity. Dev. Cell *22*, 811–823.

Hase, K., Nakatsu, F., Ohmae, M., Sugihara, K., Shioda, N., Takahashi, D., Obata, Y., Furusawa, Y., Fujimura, Y., Yamashita, T., et al. (2013). AP-1B-Mediated Protein Sorting Regulates Polarity and Proliferation of Intestinal Epithelial Cells in Mice. Gastroenterology *145*, 625–635.

Heldwein, E.E., Macia, E., Wang, J., Yin, H.L., Kirchhausen, T., and Harrison, S.C. (2004). Crystal structure of the clathrin adaptor protein 1 core. Proc. Natl. Acad. Sci. USA *101*, 14108–14113.

Hirst, J., Borner, G.H., Antrobus, R., Peden, A.A., Hodson, N.A., Sahlender, D.A., and Robinson, M.S. (2012). Distinct and overlapping roles for AP-1 and GGAs revealed by the "knocksideways" system. Curr. Biol. *22*, 1711–1716.

Klumperman, J., Hille, A., Veenendaal, T., Oorschot, V., Stoorvogel, W., von Figura, K., and Geuze, H.J. (1993). Differences in the endosomal distributions of the two mannose 6-phosphate receptors. J. Cell Biol. *121*, 997–1010.

Koivisto, U.M., Hubbard, A.L., and Mellman, I. (2001). A novel cellular phenotype for familial hypercholesterolemia due to a defect in polarized targeting of LDL receptor. Cell *105*, 575–585.

Lee, I., Doray, B., Govero, J., and Kornfeld, S. (2008). Binding of cargo sorting signals to AP-1 enhances its association with ADP ribosylation factor 1-GTP. J. Cell Biol. *180*, 467–472.

Martens, A.S., Bode, J.G., Heinrich, P.C., and Graeve, L. (2000). The cytoplasmic domain of the interleukin-6 receptor gp80 mediates its basolateral sorting in polarized madin-darby canine kidney cells. J. Cell Sci. *113*, 3593–3602.

Matter, K., Hunziker, W., and Mellman, I. (1992). Basolateral sorting of LDL receptor in MDCK cells: the cytoplasmic domain contains two tyrosine-dependent targeting determinants. Cell *71*, 741–753.

Matter, K., Whitney, J.A., Yamamoto, E.M., and Mellman, I. (1993). Common signals control low density lipoprotein receptor sorting in endosomes and the Golgi complex of MDCK cells. Cell *74*, 1053–1064.

Mattera, R., Boehm, M., Chaudhuri, R., Prabhu, Y., and Bonifacino, J.S. (2011). Conservation and diversification of dileucine signal recognition by adaptor protein (AP) complex variants. J. Biol. Chem. *286*, 2022–2030.

Odorizzi, G., and Trowbridge, I.S. (1997). Structural requirements for basolateral sorting of the human transferrin receptor in the biosynthetic and endocytic pathways of Madin-Darby canine kidney cells. J. Cell Biol. *137*, 1255–1264.

Ohka, S., Ohno, H., Tohyama, K., and Nomoto, A. (2001). Basolateral sorting of human poliovirus receptor alpha involves an interaction with the mu1B subunit of the clathrin adaptor complex in polarized epithelial cells. Biochem. Biophys. Res. Commun. *287*, 941–948.

Ohno, H., Stewart, J., Fournier, M.C., Bosshart, H., Rhee, I., Miyatake, S., Saito, T., Gallusser, A., Kirchhausen, T., and Bonifacino, J.S. (1995). Interaction of tyrosine-based sorting signals with clathrin-associated proteins. Science *269*, 1872–1875.

Ohno, H., Fournier, M.C., Poy, G., and Bonifacino, J.S. (1996). Structural determinants of interaction of tyrosine-based sorting signals with the adaptor medium chains. J. Biol. Chem. *271*, 29009–29015.

Ohno, H., Tomemori, T., Nakatsu, F., Okazaki, Y., Aguilar, R.C., Foelsch, H., Mellman, I., Saito, T., Shirasawa, T., and Bonifacino, J.S. (1999). Mu1B, a novel adaptor medium chain expressed in polarized epithelial cells. FEBS Lett. *449*, 215–220.

Pathak, R.K., Yokode, M., Hammer, R.E., Hofmann, S.L., Brown, M.S., Goldstein, J.L., and Anderson, R.G. (1990). Tissue-specific sorting of the human LDL receptor in polarized epithelia of transgenic mice. J. Cell Biol. *111*, 347–359.

Peden, A.A., Oorschot, V., Hesser, B.A., Austin, C.D., Scheller, R.H., and Klumperman, J. (2004). Localization of the AP-3 adaptor complex defines a novel endosomal exit site for lysosomal membrane proteins. J. Cell Biol. *164*, 1065–1076.

Ren, X., Farías, G.G., Canagarajah, B.J., Bonifacino, J.S., and Hurley, J.H. (2013). Structural basis for recruitment and activation of the AP-1 clathrin adaptor complex by Arf1. Cell *152*, 755–767.

Robinson, M.S. (1990). Cloning and expression of gamma-adaptin, a component of clathrin-coated vesicles associated with the Golgi apparatus. J. Cell Biol. *111*, 2319–2326.

Robinson, M.S. (2004). Adaptable adaptors for coated vesicles. Trends Cell Biol. *14*, 167–174.

Robinson, M.S., and Kreis, T.E. (1992). Recruitment of coat proteins onto Golgi membranes in intact and permeabilized cells: effects of brefeldin A and G protein activators. Cell *69*, 129–138.

Schreiner, R., Frindt, G., Diaz, F., Carvajal-Gonzalez, J.M., Perez Bay, A.E., Palmer, L.G., Marshansky, V., Brown, D., Philp, N.J., and Rodriguez-Boulan, E. (2010). The absence of a clathrin adapter confers unique polarity essential to proximal tubule function. Kidney Int. *78*, 382–388.

Stamnes, M.A., and Rothman, J.E. (1993). The binding of AP-1 clathrin adaptor particles to Golgi membranes requires ADP-ribosylation factor, a small GTP-binding protein. Cell *73*, 999–1005.

Sugimoto, H., Sugahara, M., Fölsch, H., Koide, Y., Nakatsu, F., Tanaka, N., Nishimura, T., Furukawa, M., Mullins, C., Nakamura, N., et al. (2002).

Differential recognition of tyrosine-based basolateral signals by AP-1B subunit mu1B in polarized epithelial cells. Mol. Biol. Cell *13*, 2374–2382.

Takahashi, D., Hase, K., Kimura, S., Nakatsu, F., Ohmae, M., Mandai, Y., Sato, T., Date, Y., Ebisawa, M., Kato, T., et al. (2011). The epithelia-specific membrane trafficking factor AP-1B controls gut immune homeostasis in mice. Gastroenterology *141*, 621–632.

Traub, L.M., Ostrom, J.A., and Kornfeld, S. (1993). Biochemical dissection of AP-1 recruitment onto Golgi membranes. J. Cell Biol. *123*, 561–573.

Wang, Y.J., Wang, J., Sun, H.Q., Martinez, M., Sun, Y.X., Macia, E., Kirchhausen, T., Albanesi, J.P., Roth, M.G., and Yin, H.L. (2003). Phosphatidylinositol 4 phosphate regulates targeting of clathrin adaptor AP-1 complexes to the Golgi. Cell *114*, 299–310.

Wong, D.H., and Brodsky, F.M. (1992). 100-kD proteins of Golgi- and trans-Golgi network-associated coated vesicles have related but distinct membrane binding properties. J. Cell Biol. *117*, 1171–1179.